INNSPUB

Journal of Biodiversity and Environmental Sciences (JBES)
ISSN: 2220-6663 (Print) 2222-3045 (Online)
Vol. 22, No. 6, p. 177-184, 2023
http://www.innspub.net

RESEARCH PAPER OPEN ACCESS

Synthesis and evaluation of chitosan nanoparticle doped activated carbon (CSNPs@AC) as a photocatalyst to earn the degradation of organic dye

T. Shanmugavadivu[1], P. Bhuvaneswari[1], G. Sabeena[2], G. Annadurai[2], E. Pushpalakshmi[2], S. Rajaduraipandian[1], E. Sindhuja[*1]

[1]*Department of Chemistry, Sri Paramakalyani College, Manonmaniam Sundaranar University, Alwarkurichi, Tamil Nadu, India*

[2]*Sri Paramakalyani Centre of Excellence in Environmental Sciences, Manonmaniam Sundaranar University, Alwarkurichi, Tamil Nadu, India*

Article published on June 15, 2023

Key words: Chitosan nanoparticle, Activated carbon, Malachite green, XRD, UV, FT-IR, SEM-EDX

Abstract

Growing human and industrial activity causes organic contaminants like dyes to contaminate water resources. This study created a nanocomposite photocatalyst for the breakdown of organic dye pollutants called a chitosan nanoparticle doped activated carbon (CSNPs@AC). The creation of the chitosan nanoparticle-doped activated carbon (CSNPs@AC) nanocomposite was confirmed by XRD, UV, FT-IR, and SEM-EDX studies. Using malachite green (MG) as a model organic dye, photocatalytic degradation was examined under UV and visible light. During photocatalytic degradation, it was discovered that the absorbance decreased in direct proportion to the drop in dye concentration. With MG, the degeneration happened more quickly. Additionally, the photocatalyst was more effective at degrading malachite green (MG) under UV light.

***Corresponding Author:** E. Sindhuja ✉ sindhujaelangovan@gmail.com

Introduction

Chitin, a structural macromolecule found in the exoskeletons of crustaceans and the cell walls of fungi, is converted into chitosan, the second most abundant natural polymer, by a process known as deacetylation. This polymer has advantageous qualities that make it useful as a purification agent for eliminating pollutants, including non-toxicity, antibacterial activity, biodegradability, low cost, great natural abundance, and excellent chelating characteristics. (Sahidi *et al*., 1999). Due to its special characteristics, including biodegradability, biocompatibility, and antiseptic capabilities, chitosan has gained much greater attention among polymers (Rabea *et al*., 2003; Venkatesa *et al*., 2017; Kumar, 2000). β-(1→4)-linked D-glucosamine and Nacetyl-D-glucosamine are randomly distributed throughout the linear polysaccharide known as chitosan. (Balagangadharan *et al*., 2017).

Chitosan's molecular chain contains functional groups called hydroxyl and amino, making it easier for connections to develop and allowing for the linked structures found in chitosan-based nanocomposites (Hu *et al*., 2021). Chitosan nanoparticles and composites have been integrated into studies in recent years. In the photocatalytic reactor, photocatalyst particles are exposed to light to excite electrons from the valence energy band to the conduction energy band, which results in the production of hydroxyl radicals with a high capacity for oxidation (Gholami *et al*., 2020; Hassandoost *et al*., 2019). According to (Srivastava *et al*., 2004) malachite green is a caustic, toxic, and dangerous basic dye that falls under the triphenylmethane group. Due to its potential for being carcinogenic, mutagenic, and teratogenic, it is recognized as one of the most hazardous synthetic dye pollutants (Nie and Nie 2019). Malachite green can cause infections, problems with conception, and nasal and mouth irritation (Kanhere *et al*., 2014). According to (Culp and Beland, 1996) it is also harmful to the gills, kidneys, intestines, and liver, leading to organ damage, developmental abnormalities, and carcinogenic illnesses. Malachite green has several commercial uses, but it is also frequently used to dye cotton, plastics, wool, paper, and silk (Roy *et al*., 2020). Malachite green dye contamination of groundwater as a result of inappropriate discharge of effluents from such enterprises is thus a severe issue that requires careful attention. Degradation is more appropriate among these strategies due to its simplicity of design, ease of operation, efficacy, high efficiency, and accessibility to a wide spectrum of degradation (Zhao *et al*., 2011; Tewari *et al*., 2018). Consequently, distinctive degradation such as biomass, (Tsai and Chen, 2010; Sarojini *et al*., 2022) activated carbon (AC) (Tang *et al*., 2020; Altintig *et al*., 2018; Naushad *et al*., 2019) and metal oxides and their composites (Zhou *et al*., 2011; Rajabi *et al*., 2019; Shamsizadeh *et al*., 2014; Wang *et al*., 2015) suffer from become to remove malachite green dyes from water. Due to their vast active sites, porous architectures, high surface areas, thermal stability, ease of recovery, and low toxicity, metal oxide nanoparticles stand out among other adsorbents in terms of potential and performance (Kumar *et al*., 2013; Nagpal and Kakkar *et al*., 2019).

In the current study, chitosan nanoparticle-doped activated carbon (CSNPs@AC) polymer nanocomposites were prepared. Nanocomposites of CSNPs@AC Characterized by FTIR (Fourier Transform Infrared Spectroscopy), XRD (X-Ray Diffraction), UV (Ultra Violet Spectroscopy), and SEM-EDX (Scanning Electron Microscopy-EDX) were investigated. Additionally, the creation and investigation of a chitosan nanoparticle doped activated carbon (CSNPs@AC) nanocomposite as a potential photocatalyst in the photodegradation of organic dyes like Malachite green (MG) are the main objectives of this study.

Materials and methods

All of the compounds used in this investigation were analytical grade and received from Merck in India. They were used directly from the source without further purification. Sigma-Aldrich sold chitosan that had undergone 80% deacetylation, along with activated carbon, acetic acid, hydrochloric acid, and

ethanol absolutely among the starting point. With distilled water, all preparatory steps were completed. The use of all analytical-grade chemicals and reagents was done before further purification.

Preparation of Chitosan Nanoparticles (CNPs)

Chitosan was weighed out, dissolved in 100 ml of 2% acetic acid solution, and stirred continuously for about two hours at room temperature using a magnetic stirrer. Next, 2g of sodium tri polyphosphate was dissolved in 200ml of distilled water, added dropwise, and frozen at 60^0C for twenty-four hours. The precipitate was then collected at the bottom and dried in a hot air oven at 40^0 C. Finally, research was conducted on the chitosan nanoparticles (CNPs) (Nguyen *et al*., 2020).

Preparation of Chitosan nanoparticle doped Activated Carbon (CSNPs@AC)

In a 2:1 ratio, chitosan nanoparticle-doped activated carbon (CSNPs@AC) was created. First, 150ml of distilled water was combined with 2g of chitosan nanoparticles and 1g of activated carbon. The mixture was then shaken vigorously for two days. The particle was finally settled, the solution was filtered using Whatman No. 1 filters paper, dried in a hot air oven for 24 hours at 60^0C, and then was calcined for 4 hours at 600^0C. chitosan nanoparticle doped activated carbon (CSNPs@AC) was created at the end (Nguyen *et al*., 2020).

Application of prepared Chitosan nanoparticle doped Activated Carbon (CSNPs@AC)

Photodegradation procedure

Utilizing the photocatalytic degradation of Malachite Green (MG) as a reaction probe in a beaker with stirring, the photocatalytic activity of chitosan nanoparticle doped activated carbon (CSNPs@AC) is evaluated. In order to conduct photocatalytic studies, 100 ml of solution Malachite Green (MG) from Scheme 1 was added to the reactors along alongside the necessary catalyst. To achieve the process of adsorption equilibration of the framework, the solution was nicely blended in darkness for 10 min before to irradiation. Testing samples were taken at various time intervals following UV lamp irradiations, filtered, and then added to a quartz cell. At various periods, the Malachite Green (MG) content was assessed using a UV spectrophotometer set at λ = 620nm. At ambient temperature, all photocatalytic processes were carried out. The following equation was used to compute the photodegradation efficiency:

$$\text{Photodegradation efficiency (\%)} = \frac{Co - Ce}{Co} \times 100$$

where Ce represents the final dye concentration after UV-light exposure and C_o represents the beginning dye concentration (Owda *et al*., 2021).

Characterisation

With a Nicolet Magma 550 series II, manufactured by Midac in the USA, the molecular structure of the produced hybrids was examined at wavelengths between 4000 and 400 cm-1. For FTIR analysis, the dry film was crushed into discs after being ground with KBr powder. A JEOL (Japan) JSM-T300 scanning electron microscope with EDX (SEM-EDX) was used to evaluate the morphology of the samples. A JEOL JFC-110E Ion Sputter was used to apply a gold coating on the sample. XRD patterns were acquired using Cu K radiation (k = 1.540 A°), operating at 40 kV and 40 mA, using a Bruker D8 Advance diffractometer. With a detector step size of 0.02° and an angular range of 2θ =10-80°, scans were conducted. Using a UV-Vis spectrophotometer, the bioreduction of metal particles in the arrangement was detected, with a spectrum from 200 to 800nm for each example taken against cleaned water as clear. The suspension had previously been homogenized for five minutes with an ultrasonication probe.

Result and discussion

X-Ray Diffraction (XRD)

Fig. 1 shows the XRD pattern of the activated carbon doped with chitosan nanoparticles (CSNPs@AC). The diffracted peaks in Fig. 1 were 23.6°, 26.7°, and 55.9°. The results showed distinctive peaks of the Chitosan nanoparticle doped Activated Carbon (CSNPs@AC), which is proof that the polymer composite was successfully blended (Hanif *et al*., 2015; Verma *et al*., 2021) and is in good accord with other chitosan,

activated carbon diffraction peaks. Using the Debye-Scherrer formula, the specific size of the crystallites was determined to be 65nm, which is in the nanometric range.

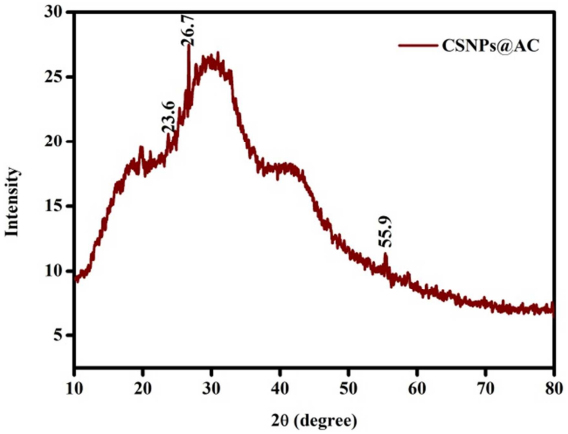

Fig. 1. The XRD graph of Chitosan nanoparticle doped Activated Carbon (CSNPs@AC).

Fourier Transform Infrared Spectroscopy (FTIR)

The bands seen for chitosan nanoparticles at 461 cm^{-1} are attributed to many C-OH groups and C-NH_2 groups. According to (Peternel *et al.*, 2007) the bands at 448 cm^{-1} belong to a combinational vibration band connected to chitin rings.

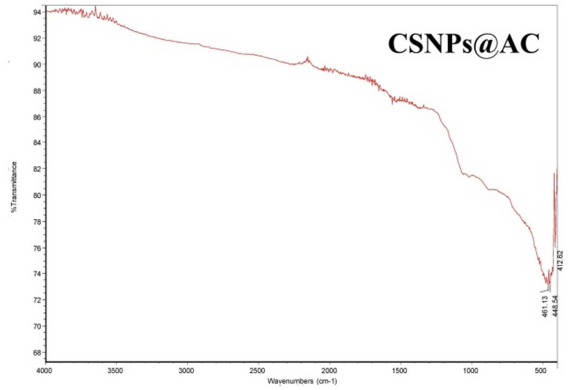

Fig. 2. The FTIR graph of Chitosan nanoparticle doped Activated Carbon (CSNPs@AC).

These peaks showed that chemical processes, such as the formation of hydrogen bonds between the oxygen groups of the activated carbon and the functional groups of the chitosan nanoparticles, were in charge of the successful grafting of the activated carbon with chitosan nanoparticles (Sharififard *et al.*, 2018; Farahmandjou *et al.*, 2015). A band that appears at 412 cm^{-1} for the activated carbon materials doped with chitosan nanoparticles (CSNPs@AC) is attributable to N-H stretching vibrations. Activated carbon materials doped with chitosan nanoparticles (CSNPs@AC) are presented in their FTIR spectrum and data are shown in Fig. 2.

Scanning Electron Microscopy-EDX (SEM-EDX)

The morphological traits of the activated carbon materials that were doped with chitosan nanoparticles (CSNPs@AC) and subjected to SEM analysis are shown in Fig. 3.

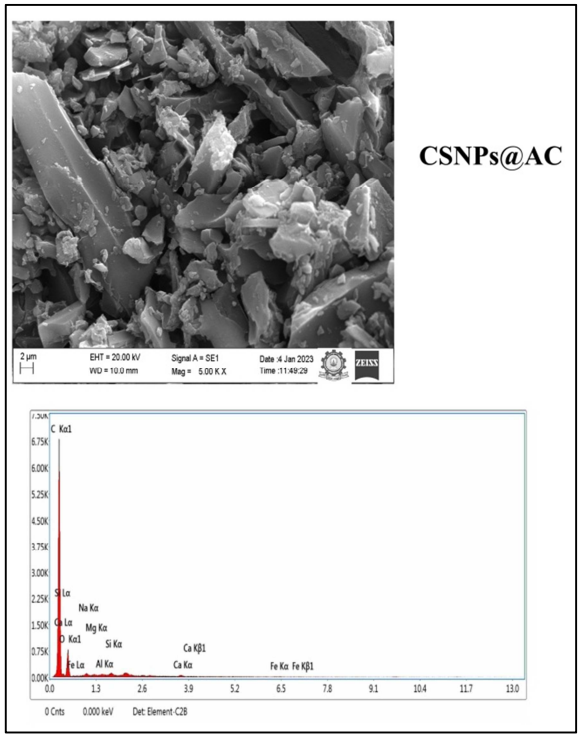

Fig. 3. The SEM-EDX graph of Chitosan nanoparticle doped Activated Carbon (CSNPs@AC).

In response to the SEM-EDX of the activated carbon materials doped with chitosan nanoparticles (CSNPs@AC), the activated carbon materials doped with chitosan nanoparticles (CSNPs@AC) cooperation into identical fragmented porosity shape is due to the homogeneous dispersion of chitosan nanoparticles in the activated carbon materials doped with chitosan nanoparticles (CSNPs@AC). We looked at the components that made up the CSNPs@AC. The SEM-EDX spectrum is depicted in various locations

in Fig. 3. The peaks that are visible are C, Ca, Si, O, Fe, Al, and Mg, respectively. Activated carbon composites that have been doped with chitosan nanoparticles (CSNPs@AC) clearly include both polymer and activated carbon. (Rathore *et al.*, 2020)

Ultra Violet Spectroscopy (UV)

The UV-Vis spectra of the compound-activated carbon doped with chitosan nanoparticles (CSNPs@AC) are shown in Fig. 4. Chitosan nanoparticles doped activated carbon (CSNPs@AC) exhibit an electronic transition at a wavelength of 274nm. The (n-π*) transition has been proposed to be the mechanism of a factor in the absorption peak significance, which ranges from 250 to 520nm (Singh Rathore *et al.*, 2022). The existence of activated carbon in the activated carbon doped with chitosan nanoparticles (CSNPs@AC) is responsible for this electrical shift.

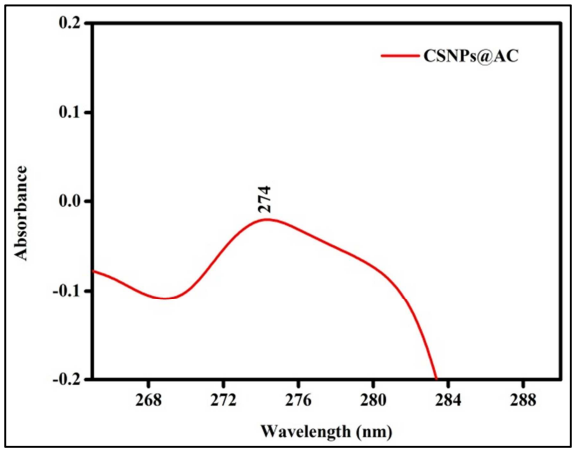

Fig. 4. The UV graph of Chitosan nanoparticle doped Activated Carbon (CSNPs@AC).

Mechanism of Photodegradation Activity

In Scheme 1, the breakdown of the malachite green dye is shown to be a light-dependent process. During this procedure, a positive hole, h+, is raised within the valence band, and the dye is initially adsorbed on the catalyst's surface (CSNPs@AC). After that, UV light is used to stimulate the dye's valence electrons and cause them to move from the valence band to the conduction band. Adsorbed water molecules react with positive holes and free electrons on the surface of the photocatalyst to form OH radicals, while free electrons transform dissolved oxygen into superoxide anion O_2 radicals. These light-generated radicals degrade the dye molecules into less complex compounds like CO_2 and H_2O. (Ajmal *et al.*, 2014).

$$CSNPs@AC + h\nu \rightarrow e- + h^+ \quad (1)$$

$$H_2O + h+ \rightarrow OH^{\cdot} + H^+ \quad (2)$$

$$O_2 + e^- \rightarrow O_2^{\cdot -} \quad (3)$$

$$OH + MG\ dye \rightarrow degradable\ product \quad (4)$$

$$O_2- + dye \rightarrow degradable\ product \quad (5)$$

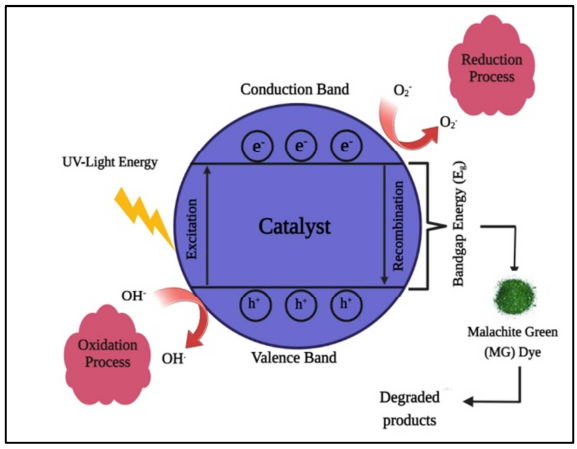

Scheme 1. Reaction mechanisms for the degradation of Malachite Green (MG).

Photocatalytic Activity

The activated carbon materials doped with chitosan nanoparticles (CSNPs@AC) components will first be tested individually before being analyzed collectively to determine the viability of improving the catalytic performance. Fig. 5(A, B) illustrates the photodegradation efficiency of several activated carbon materials doped with chitosan nanoparticles (CSNPs@AC) illumination times during a 90-minutes period. The activated carbon materials doped with chitosan nanoparticles (CSNPs@AC) showed increased photocatalytic capacity during UV light radiation treatment. This specific occurrence is believed to be caused by the higher degree of interphase contact that can be obtained at activated carbon materials doped with chitosan nanoparticles (CSNPs@AC) (Dai *et al.* 2013; Sabeena *et al.*, 2023). The results showed that increasing the number of activated carbon materials doped with chitosan nanoparticles (CSNPs@AC) at first increased the rate

of photodegradation of Malachite Green, but beyond a certain point, it decreased and the exposed surface area of the photocatalyst increased as well. The upper limit of the saturation point was reached by the activated carbon doped with chitosan nanoparticles (CSNPs@AC), as shown in Fig. 5(A, B), and increasing the amount led to less dye degradation after that.

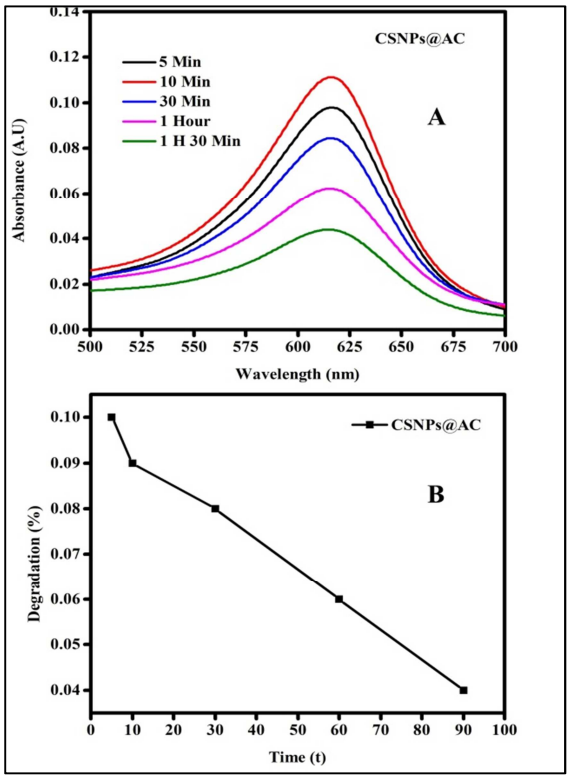

Fig. 5. The Photocatalytic graph of Chitosan nanoparticle doped Activated Carbon (CSNPs@AC) (a) represents Chitosan nanoparticle doped Activated Carbon (CSNPs@AC) (b) represents the degradation of dye from Chitosan nanoparticle doped Activated Carbon (CSNPs@AC).

Conclusion

The effective synthesis and characterization of a chitosan nanoparticle doped activated carbon (CSNPs@AC) photocatalyst using XRD, UV, FT-IR, and SEM-EDX studies. Malachite green (MG), a model organic pollutant, was shown to be destroyed by chitosan nanoparticle doped activated carbon (CSNPs@AC) in photocatalytic activity experiments when exposed to UV-visible light. Under UV lighting, it was discovered that chitosan nanoparticle-doped activated carbon (CSNPs@AC) was more photoresponsive. Additionally, the photocatalyst for the breakdown of malachite green (MG) was more effective when chitosan nanoparticle doped activated carbon (CSNPs@AC).

References

Ajmal A, Majeed I, Malik RN, Idriss H, Nadeem MA. 2014. Principles and mechanisms of photocatalytic dye degradation on TiO_2 based photocatalysts: a comparative overview. RSC Advances **4(70),** 37003-37026.

Altintig E, Onaran M, Sarı A, Altundag H, Tuzen M. 2018. Preparation, characterization and evaluation of bio-based magnetic activated carbon for effective adsorption of malachite green from aqueous solution. Materials Chemistry and Physics **220,** pp.313-321.

Balagangadharan K, Dhivya S, Selvamurugan N. 2017. Chitosan based nanofibers in bone tissue engineering. International journal of biological macromolecules **104,** 1372-1382.

Culp Sandra, Beland Frederick. 1996. Malachite Green: A Toxicological Review. International Journal of Toxicology **15(3),** 219-238.

Dai K, Zhang X, Fan K, Peng T, Wei B. 2013. Hydrothermal synthesis of single-walled carbon nanotube-TiO2 hybrid and its photocatalytic activity. Applied Surface Science **270,** 238-244.

Farahmandjou, M, Soflaee F. 2015. Synthesis and characterization of α-Fe_2O_3 nanoparticles by simple co-precipitation method. Phys. Chem. Res **3,** 191-196.

Gholami P, Khataee A, Soltani RDC, Dinpazhoh L, Bhatnagar A. 2020. Photocatalytic degradation of gemifloxacin antibiotic using Zn-Co-LDH@ biochar nanocomposite. Journal of hazardous materials **382,** 121070.

Hanif NSM, Shahril NSM, Azmar A, Winie T. 2015. Studies on the effect of acid treated TiO_2 on the electrical and tensile properties of hexanoyl chitosan-polystyrene-$LiCF_3SO_3$ composite polymer electrolytes. In AIP Conference Proceedings **1674(1),** 020028.

Hassandoost R, Pouran SR, Khataee A, Orooji Y, Joo SW. 2019. Hierarchically structured ternary heterojunctions based on Ce^{3+}/Ce^{4+} modified Fe_3O^4 nanoparticles anchored onto graphene oxide sheets as magnetic visible-light-active photocatalysts for decontamination of oxytetracycline. J. Hazard. Mater **376,** 200-211.

Hu B, Guo Y, Li H, Liu X, Fu Y, Ding F. 2021. Recent advances in chitosan-based layer-by-layer biomaterials and their biomedical applications. Carbohydrate Polymers **271,** 118427.

Kanhere J, Gopinathan R, Banerjee J. 2014. Cytotoxicity and genotoxicity of malachite green on non-target aquatic organisms: Chlorella pyrenoidosa and Daphnia magna. Water, Air, & Soil Pollution **225,** 1-8.

Kumar KY, Muralidhara H, Nayaka YA, Balasubramanyam J, Hanumanthappa H. 2013. Low-cost synthesis of metal oxide nanoparticles and their application in adsorption of commercial dye and heavy metal ion in aqueous solution Powder Technol **246,** 125-136.

Kumar MNR. 2000. A review of chitin and chitosan applications. Reactive and functional polymers **46(1),** 1-27.

Nagpal M, Kakkar R. 2022. The selective removal of Congo red using dumbbell-shaped hierarchically porous Ca-Mg mixed oxide. Applied Surface Science Advances **8,** 100221.

Nguyen NT, Nguyen NT, Nguyen VA. 2020. In Situ Synthesis and Characterization of ZnO/Chitosan Nanocomposite as an Adsorbent for Removal of Congo Red from Aqueous Solution. Advances in Polymer Technology **20,** 1-8.

Nie Q, Nie S. 2019. High-performance liquid chromatography for food quality evaluation. In Evaluation Technologies for Food Quality 267-299.

Owda ME, Elfeky AS, Abouzeid RE, Saleh AK, Awad MA, Abdellatif HA, Ahmed FM Elzaref AS. 2021. Enhancement of photocatalytic and biological activities of chitosan/activated carbon incorporated with TiO_2 nanoparticles. Environmental Science and Pollution Research **29,** 18189-18201.

Peternel IT, Koprivanac N, Bozic AML, Kusic HM. 2007. Comparative study of UV/TiO_2, UV/ZnO and photo-Fenton processes for the organic reactive dye degradation in aqueous solution. J. Hazard Mater **148(12),** 477-484.

Rabea EI, Badawy MET, Stevens CV, Smagghe G, Steurbaut W. 2003. Chitosan as antimicrobial agent: applications and mode of action. Biomacromolecules **4,** 1457-1465.

Rajabi M, Kazem Mahanpoor, Moradi O. 2019. Preparation of PMMA/GO and PMMA/GO-Fe_3O_4 nanocomposites for malachite green dye adsorption: Kinetic and thermodynamic studies **167,** 544 555.

Rathore BS, Chauhan NPS, Rawal MK, Ameta SC, Ameta R. 2020. Chitosan-polyaniline-copper (II) oxide hybrid composite for the removal of methyl orange dye. Polym. Bull. **77,** 4833-4850.

Roy DC, Biswas SK, Sheam MM. 2020. Bioremediation of malachite green dye by two bacterial strains isolated from textile effluents. Current Research in Microbial Sciences **49,** 1-20.

Sabeena G, Vainath Praveen S, Pushpalakshmi E, Annadurai, G. 2023. Comparative synthesis and characterization of nanocomposites using chemical and green approaches including a comparison study on in vivo and in vitro biological properties. Nanoscale Advances **5,** 767-785

Sarojini G, Babu SV, Rajamohan N, Rajasimman M. 2022. Performance evaluation of polymer-marine biomass-based nanocomposite for the adsorptive removal of malachite green from synthetic wastewater. Environmental Research **204,** 112-132.

Shahidi F, Arachchi JKV, Jeon YJ. 1999. Food applications of chitin and chitosan. Trends in food science & technology **10(2),** 37-51.

Shamsizadeh A, Mehrorang Ghaedi, Ansari, AA, Azizian S, Mihir Kumar Purkait. 2014. Tin oxide nanoparticle loaded on activated carbon as new adsorbent for efficient removal of malachite green-oxalate: Non-linear kinetics and isotherm study **195,** 212-218.

Sharififard H, Rezvanpanah E, Rad SH. 2018. A novel natural chitosan/activated carbon/iron bionanocomposite: Sonochemical synthesis, characterization, and application for cadmium removal in batch and continuous adsorption process. Bioresour Technol **270,** 562-569.

Singh Rathore B, Pal Singh Chauhan N, Panneerselvam P, Jadoun S, Barani M, Ameta SC, Ameta R. 2022. Synthesis and Characterization of Ch-PANI-Fe2O3 Nanocomposite and Its Water Remediation Applications. Water **14(22),** 3615.

Srivastava S, Sinha R, Roy D. 2004. Toxicological effects of malachite green. Aquatic Toxicology **66(3),** 319-329.

Tang SH, Ahmad Zaini MA. 2020. Development of activated carbon pellets using a facile low-cost binder for effective malachite green dye removal. Journal of Cleaner Production **253,** 119970.

Tewari K, Singhal G, Arya RK. 2018. Adsorption removal of malachite green dye from aqueous solution. Rev. Chem. Eng **34,** 427-453

Tsai WT, Chen HR. 2010. Removal of malachite green from aqueous solution using low-cost chlorella-based biomass. J Hazard Mater **15,** 1-3.

Venkatesan J, Anil S, Kim SK, Shim MS. 2017. Chitosan as a vehicle for growth factor delivery: various preparations and their applications in bone tissue regeneration. Int. J. Biol. Macromol **104,** 1383-1397.

Verma DK, Malik R, Meena J, Rameshwari R. 2021. Synthesis, characterization and applications of chitosan based metallic nanoparticles: A review. Journal of Applied and Natural Science **13(2),** 544-551.

Wang D, Liu L, Jiang X. 2015. Adsorption and removal of malachite green from aqueous solution using magnetic β-cyclodextrin-graphene oxide nanocomposites as adsorbents. Colloids Surf Physicochem Eng Asp **466,** 166-173.

Zhao X, Lv L, Pan B, Zhang W, Zhang S, Zhang Q. 2011. Polymer-supported nanocomposites for environmental application: A review. Chemical Engineering Journal **170,** 381-394.

Zhou L, Jin J, Liu Z, Liang X, Shang C. 2011. Adsorption of acid dyes from aqueous solutions by the ethylenediamine-modified magnetic chitosan nanoparticles. Journal of Hazardous Materials **185,** 1045-1052.